Drying Shrinkage and Cracking Tendency of Concrete Pavement Mixtures with Variable Packing Densities of Aggregates and Paste Contents

Jan Olek[1,*], and *Adam* Rudy[2]

[1]Purdue University, Lyles School of Civil Engineering, West Lafayette, IN 47907, USA
[2]LafargeHolcim Innovation Center, 38291 Saint-Quentin Fallavier, France

Abstract. Excessive drying shrinkage, and associated cracking, can lead to serious durability problem in concrete pavements and bridges. In the course of this study, the magnitude of drying shrinkage and cracking potential was evaluated for several concrete pavement mixtures as a function of packing density of the aggregate and paste contents. The results indicated that both, the shrinkage and the cracking potential depend on the volume of voids between aggregate particles (packing density), paste content of concrete mixture, and the paste-aggregate void saturation ratio.

1 Introduction and technical background

In addition to lowering the cost, the main role of aggregate in concrete is to restrain the shrinkage of the cement paste and thus to reduce the likelihood of cracking. The primary type of shrinkage encountered in elements with high surface-to-volume ratios, such as concrete pavements, is the drying shrinkage, the result of moisture loss from the exposed surface [1-5]. Assuming that the pavement is constructed from concrete utilizing good quality, dimensionally stable aggregate, the extent of drying shrinkage will be primarily controlled by the amount of cement paste. The quantity of paste present in a given mixture is, in turn, a function of the volume of voids in the aggregate skeleton (i.e. it is directly linked to the aggregate packing density [6-10]).

The research presented in this paper is a fragment of a much larger study on optimization of mixture proportions for pavement concrete that examined the influence of several factors, including the use of binary and ternary binders, paste content and the gradation of aggregates [11, 12], That study was conducted in order to explore the potential to transition from prescriptive to performance-based specifications for concrete pavements. An essential part of such transition process would be the ability to optimize the composition of concrete mixtures to enhance the performance characteristics of pavements, especially with respect to durability.

To meet this objective, concrete mixtures used in the study described in the current paper were designed using the concepts of the "air-free" paste-aggregate void saturation ratio (k")

* Corresponding author: olek@purdue.edu

and the packing density of aggregates (ϕ). Similar concepts have been used in the other studies [4, 8].

The packing density of aggregate is defined [8, 13] as the fraction of the solid volume of aggregate in the unit volume and can be calculated from Equation (1):

$$Packing\ density\ (\phi) = \frac{\rho_{aggr\ bulk}}{\rho_{aggr\ particle}} \quad (1)$$

Where: $\rho_{aggr\ bulk}$ is the bulk density of the aggregate in the compacted or loose condition and $\rho_{aggr\ particle}$ is the specific gravity of the aggregate particles.

The paste-aggregate void saturation ratio (paste-to-voids volume ratio) is defined as a fraction of the volume of the voids in the aggregate skeleton filled by the "air-free" paste and can be calculated from Equation (2) [13]:

$$k'' = \frac{V_{paste} - V_{air}}{1-\phi} \quad (2)$$

Where: V_{paste} and V_{air} are, respectively volumes of the paste and volume of the air voids.

2 Materials and methods

2.1 Materials

The components of the cementitious system used in the study included the ASTM C150 compliant Type I Portland cement and the ASTM C618 compliant Class C fly ash with specific gravity (SG) of 2.56. Locally available natural siliceous sand (SG_{SSD} = 2.66 and absorption 1.27%), meeting the gradation requirements of the Indiana Department of Transportation (INDOT) specification for #23 material [14] was used as fine aggregate. The coarse aggregates (CA) used consisted of two different gradations of crushed limestone with saturated surface dry specific gravity (SG_{SSD}) of 2.64 and absorption of 1.30%. The first gradation met the requirements of INDOT's specification for #8 stone [14] (maximum size of 25 mm) while the second gradation met the requirements of INDOT's specification for #11 stone [14] (maximum size of 12.5 mm). In order to eliminate batch-to-batch variations all coarse aggregates where sieved and recombined prior to mixing.

As already mentioned in Section 1, the variables selected for this study included the combined aggregate packing density (ϕ) and the air free paste-aggregate voids saturation ratio (k"). The rages of these two experimental variables were selected based on the results of simulations of packing densities for two and three-components aggregate blends (details can be found in [11, 12] and review of the relevant technical literature [6-10]. Based on these inputs, the selected ranges for the study variables were as follows:

- Packing density (ϕ) (from 0.715 to 0.786)
- Paste-aggregate void saturation ratio (k") (from 0.869 to 1.018)

The ranges of variables listed above were used as inputs for the 2^k factorial central composite experiment design model [15] to develop a matrix of mixtures for the study. The resulting test matrix is summarized in Table 1.

Table 1. Matrix of mixtures based on central factorial design of experiment**.**

Coded values		Uncoded values	
Packing density, ϕ	**Paste-to void saturation ratio, k"**	**Packing density, ϕ**	**Paste-to void saturation ratio, k"**
0	1.414	0.751	1.081
0	0	0.751	0.975
1	1	0.776	1.050
-1	1	0.726	1.050
1	-1	0.776	0.900
1.4142	0	0.786	0.975
-1	-1	0.726	0.900
0	-1.414	0.751	0.869
-1.414	0	0.715	0.975

The combined aggregate gradations with the desired packing densities (ϕ) listed in Table 1 were developed by blending various weight proportions of #23 sand with either one or both of coarse aggregates (i.e. #8 and #11), each with its own specific version of gradation. In order to produce these specific gradations, all "as-received" aggregates (except for sand) were first dried and then they were split into individual fractions using the standard set of sieves. These fractions were then re-combined to produce a variety of blends with desired overall gradations. In total, three different versions of specific gradations were produced for #11 CA and five different versions of specific gradations were produced for #8 CA (details can be found in [11])

A total of five different aggregate blends were needed to cover the entire range of desired packing densities. The specifics of these blends are listed in Table 2. The labeling system employed to identify the specific blends uses the following notation: CA1size.gradation version_(if used) CA2size.gradation version_Sand_(P) packing density_Packing density value. As an example, #8.5_11.2-23_P_0.786 identifies the aggregate blend prepared by mixing #8CA (specific gradation version 5) with #11CA (specific gradation 2) and #23 sand with final packing density of 0.786.

Table 2. Composition of individual aggregate blends and resulting packing densities.

Aggregate Blend	CA1 (#8), % of total mass	CA2 (#11), % of total mass	Sand (#23), % of total mass	Packing density (ϕ)
#8.5_11.2_23_0.786	43.1	20.8	36.1	0.786
#8.2_23_0.726	73.4		26.6	0.726
#8.1_11.1_23_0.751	42.2	20.3	37.5	0.751
#8.4_11.3_23_0.776	44.1	20.9	35.0	0.776
#8.5_23_0.715	69.6		30.4	0.715

The values of the packing densities shown in Table 2 were calculated using Eq (1). It should also be noted, that the values of these packing densities will depend on the degree of compaction of the aggregate skeleton. In this study, the packing densities of aggregate blends were obtained following the standard rodding procedure outlined in ASTM C29.

Figure 1 shows the locations of gradations listed in Table 2 on three charts commonly used for selection of the optimized gradations of the aggregates. These charts include the "8-18" chart (Figure 1(a)), the 0.45 power chart (Figure 1 (b)) and the Shilstone workability-coarseness chart [16] (Figure 1 (c)). It could be seen (Figure 1(a)) that gradations with high packing densities (0.786 and 0.776) are essentially located within the recommended [17] "8-

18" limits . Two other gradations (with packing densities of 0.726 and 0.715) represent gap-graded blends whereas the last gradation (with packing density of 0.751) contains excessive amount of material retained at 4.75 mmm sieve.

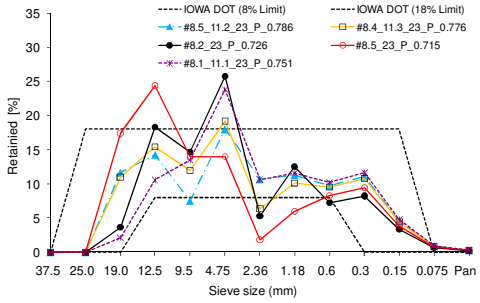

(a)

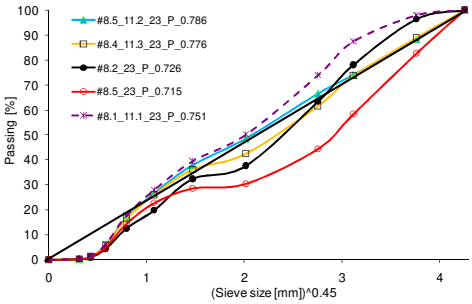

(b)

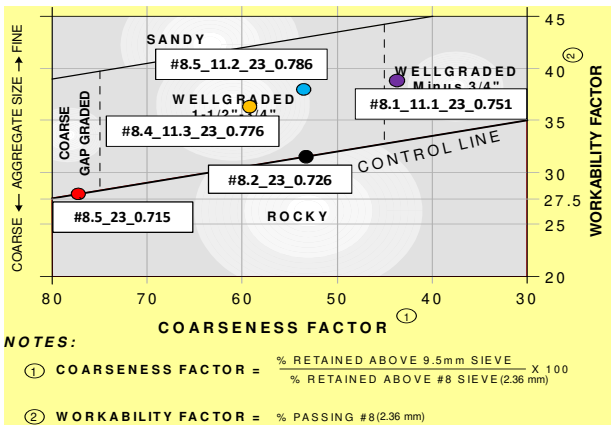

(c)

Fig. 1. Combined aggregate gradations shown on: (a) 8-to-18chart, (b), 0.45 power chart, and (c) Shilstone workability-coarseness chart.

Figure 1(b) illustrates that aggregate gradations with high packing density follow the maximum density line (MDL), whereas the gap graded ones stay below or meander along the MDL. The aggregate blend with $\phi = 0.751$ can be characterized an "intermediate" gradation between well and gap-graded blends since it stays above but also close to the MDL line. Finally, Figure 1(c) illustrates that aggregate blends with $\phi = 0.786$ and 0.776 are located within coarseness factor (CF) range from 55 to 65 and workability factor (WF) range from 35 to 40. These ranges were proposed by Shilstone [16] and confirmed by Richardson [17] as representing well-graded graded aggregate blends. On the other hand, aggregate blends with low packing density (0.715 and 0.726) are located in the range of CF and WF characteristic for gap-graded and "rocky" gradations. Finally, the CF and WF values for aggregate blend with $\phi = 0.751$ are located in the well-graded zone for aggregate finer than 19 mm.

2.2 Concrete mixture compositions

The selection of composition of concrete mixtures used in the study was based on the results of earlier optimization studies [11,18] which also considered practical constrains related to the amount of cementitious materials typically used on pavement projects in the state of Indiana (306 to 337 kg/m^3). Given these considerations, all mixes were designed to contain 28% of Class C fly ash as a replacement for cement (that level of fly ash was found to be the most desirable in the earlier study[11,18]). A total of 9 different mixtures were produced, each with different combination of air free paste-aggregate void saturation ratio and aggregate blend. The actual proportions of concrete mixture used, along with their slumps and air contents are given in Table 3.

Table 3. Composition, slump and air content of concrete mixtures.

Packing density	**0.715**	**0.726**	**0.726**	0.751	0.751	**0.751**	0.776	0.776	0.786
k"	**0.975**	**0.900**	**1.050**	0.869	0.975	**1.081**	0.900	1.05	0.975
Air-free paste [%]	**27.8**	**24.7**	**28.8**	21.7	24.3	**26.8**	20.2	23.6	20.9
Cement [kg/m^3]	**257**	**228**	**266**	201	224	**247**	187	218	193
Fly ash [kg/m^3]	**100**	**89**	**103**	78	87	**96**	72	85	75
Total Cement. [kg/m^3]	**357**	**317**	**369**	279	311	**343**	259	303	267
Water [kg/m^3]	**157**	**139**	**162**	123	137	**151**	114	133	118
Fine agg. [kg/m^3]	**523**	**482**	**454**	709	684	**659**	657	645	685
Coarse agg. [kg/m^3]	**1197**	**1331**	**1311**	1182	1140	**1098**	1219	1198	1229
WR[mL/100 kg	**0.0**	**84**	**0.0**	422	130	**0.0**	416	140	442
AEA [mL/100 kg]	**201**	**182**	**136**	117	117	**150**	117	137	143
w/cm	**0.44**	**0.44**	**0.44**	0.44	0.44	**0.44**	0.44	0.44	0.44
Slump (mm)	**127**	**51**	**108**	51	70	**95**	51	64	70
Air content (%)	**6.2**	**7.4**	**6.3**	6.3	6.5	**6.8**	6.4	6.7	7.0

Note: Entries in **bold** identify mixtures selected for evaluation of cracking tendency.

2.3 Shrinkage and cracking tendency testing methods

The free shrinkage measurements were conducted according to ASTM C 157 on three specimens with the dimensions of 75 x 75 x 275 mm, all prepared from a single batch of concrete.

The evaluation of the cracking tendency of concrete typically involves production of restrained concrete ring specimens and subjecting them to drying. In a typical test, only the exterior face of the ring is exposed to drying. The resulting moisture gradient induces the development of tensile stresses inside concrete. When the level of these stresses exceeds the

tensile strength of concrete, cracks start to develop inside the material. From the mechanism presented above, it is clear that the time of initiation of concrete drying will have a significant impact on the results from the ring test. In this study, the cracking tendency of concrete was evaluated using a modified procedure of the AASHTO TP34 ring test method [19] (Figure 2).

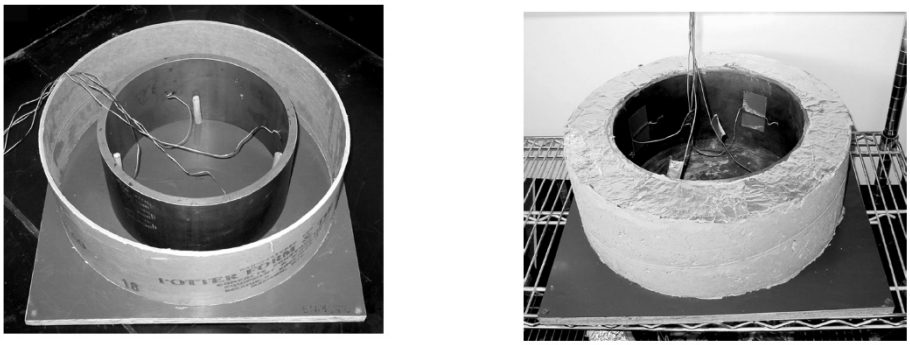

Fig. 2. Ring cracking test setup (left- empty mold; right-exposed concrete specimen cast around the steel ring (photo from [19]).

The TP34 method stipulates that that the concrete should be cured in the mold for 24 hours before the initiation of drying. In this author's opinion, this standard curing procedure may underestimate the cracking potential of concrete compared with the field conditions, where much shorter curing times (if any) may be encountered. In order to accelerate the cracking event, and to simulate potential lack of moist curing likely to be encountered under field conditions, the current study implemented modification to the standard (AASHTO PP 34-[19]) test method by initiating drying immediately after the final set time of concrete.

3 Test results

This section presents the results of the evaluation of shrinkage and cracking potential of mixes used in the study. It should be pointed out that the cracking potential was only evaluated for four of the nine mixtures used in the study (the entries for compositions and the properties of these mixtures are shown in the bold font in Table 3). The mixtures selected for the cracking potential evaluation all showed increased level of drying shrinkage, as discussed in section 3.1

3.1 Shrinkage test results

The results of free shrinkage measurements for all nine mixtures used in the study are shown in Figure 3. These results indicate that the free shrinkage depends on the packing density of aggregates (see Fig. 3(a)). Specifically, significant decrease in measured shrinkage was achieved by increasing packing density of aggregate skeleton. In addition, the positive effect of decreasing of k" value on shrinkage was also observed (see Fig. 3(b)). Generally, it seems that in order to minimize the extent of free shrinkage the mixture should have high aggregate packing density and low value of k".

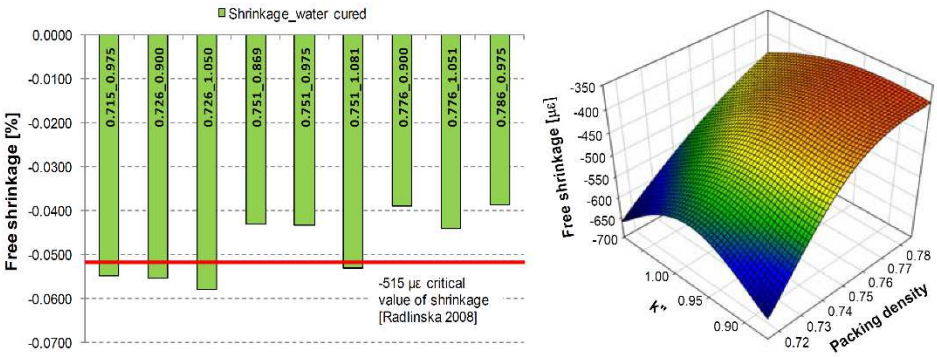

(a) (b)

Fig. 3. Free shrinkage of mixtures with different aggregate packing density (ϕ) and void saturation ratio (k"): (a) summary plot and (b) and 3D mesh plot.

3.2 Cracking tendency test results

The results of restrained shrinkage test for concrete mixtures with different aggregate packing density (ϕ) and void saturation ratio (k") are presented in Figure 4. The quantitative data, expressed as the "time-to-cracking", are given in Table 4.

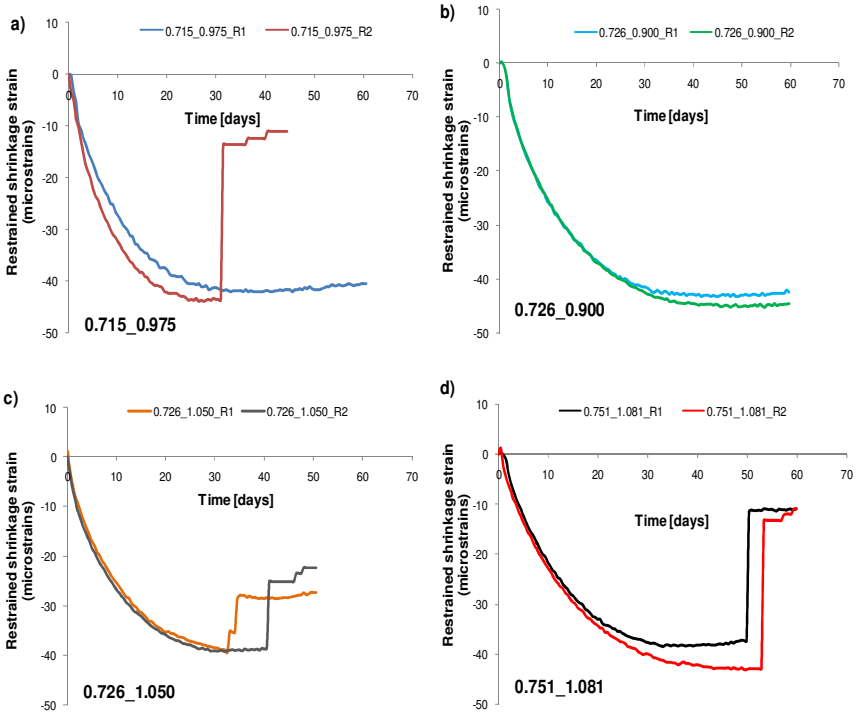

Fig. 4. The results of restrained shrinkage test for concrete mixtures with different aggregate packing density (ϕ) and void saturation ratio (k").

The first conclusion that can be derived from examining the data in Figure 4 and in Table 4 is that the time-to cracking depends primarily on the value of the paste-aggregate void saturation ratio (k") rather than on the aggregate packing density (ϕ).

Table 4. Time-to-cracking for tested concrete mixtures.

Mix	0.715_0.975	0.726_0.900	0.726_1.050	0.751_1.081
	Time-to-cracking [days]			
Ring #1	n/a	n/a	31.5	48.7
Ring #2	30.0	n/a	39.5	51.8
Average	30.0	n/a	35.5	50.3

For two concrete mixtures with highest values of the k" ratio (Fig. 4c and Fig. 4d) both ring specimens within the given group cracked at about the same time. In addition, it can also be seen that for concrete mixture with k" ratio lower than 1.0 either only one of the rings cracked (see Fig. 4a) or did not crack at all (Fig. 4b).

The "time-to-cracking" also appears to be related to the total amount of paste used to produce concrete mixtures subjected to restrained shrinkage test. By correlating the time-to-cracking data from Table 4 with the total paste content in these mixtures listed in Table 3, it can be clearly seen that mixture 0.726_1.050 containing 28.8% of paste cracked earlier than mixture 0.751_1.081, which contained 26.8% of paste.

Finally, it is interesting to note that there seem to be only limited correlation between free shrinkage and the cracking potential data. Referring to Fig. 3, it can be observed that mixtures 0.715_0.975, 0.726_0.900 and 0.726_1.050 all experienced similar amounts of free shrinkage. However, the cracking tendency for these mixtures was completely different. Mixtures 0.726_1.050 and 0.715_0.975 developed cracks, whereas mixture 0.726_0.900 did not crack at all. Based on these observations, it seems important to evaluate both, the cracking tendency and the free shrinkage in parallel in order to better evaluate potential volumetric stability problems of concrete.

4 Conclusions

The results presented in this paper lead to the following conclusions:

- durability related properties (i.e. shrinkage and cracking tendency) can be corelated with the volume of voids between aggregate particles (packing density) and paste content of concrete mixture.
- The decrease in the paste-aggregate voids saturation ratio (k" value) was found to reduce drying shrinkage.
- The results also indicated that concrete mixtures rich in paste and (at the same time) characterized by high k" value are prone to cracking. Mixtures with k" value above 1.0 cracked after 35.5 and 50.3 days after initiation of drying. On the other hand, mixture 0.726_0.900 which contained low (24.7%) amount of paste and low k" value did not crack at all.

The authors gratefully acknowledge the support of this research by the Joint Transportation Research Program administered by the Indiana Department of Transportation and Purdue University. The content of this paper reflects the views of the authors, who are responsible for the facts and the accuracy of the data presented herein, and does not necessarily reflect the official views or policies of the Federal Highway Administration and the Indiana Department of Transportation, nor do the content constituents a standard, specification, or regulation.

.

References

1. X. Wang, K. Wang, F. Bektas, P. Taylor, J. Sust. Cem. Based Mat. **1**, 56-66 (2012)
2. P. L. Ng, A. K. H. Kwan, Can. J. Civ. Eng. **43**, 875-888 (2016)
3. Y. Deshpande, J. E. Hiller, C. J. Shorkey, *Proc. Int. Symp. Brittle Matrix Composites 9*, (IFTR and Woodhead Publ. 310-312, 2009)
4. E. Yurdakul, P. C. Taylor, H. Ceylan, F. Bektas, J. Mater. Civ. Eng. **25**. 1840-1851 (2013)
5. W. M. Hale, S. F. Freyne, T. D. Bush, B. W. Russell, Constr. Build. Mater. **22**, 1990-2000 (2008)
6. D. Mostofinejad, M. Reisi. Constr. Build. Mater. **35**, 414-420 (2012)
7. W. Lindquist, D. Darwin, J. Browning, H. A. K. McLeod, J. Yuan, Constr. Build. Mater. **74**, 49-56 (2015)
8. K. Sobolev, M. Moini, S. Cramer, I. Flores-Vivian, S. Muzenski, R. Pradoto, A. Faheem, L. Phan, M. Kozhukhova, *Report No. WHRP 0092-13-04* (WisDOT, 2015).
9. T. Ley, D. Cook, G. Fick, *Part of DTFH61-06-H-00011 Work Plan 25* (National CP Tech Center, 2012)
10. N. Raj, S. G. Patil, B. Bhattacharjee, IOSR-JMCE, **11**, 34-46 (2014)
11. A. Rudy, *Ph.D. Thesis*, (Purdue University, 2009)
12. A. Rudy, J. Olek, *Publication FHWA/IN/JTRP-2012/34*, (Purdue University, 2012)
13. S. Jacobsen, B. Arntsen, Mater. Struct., **41**, 703-716 (2008)
14. Section 900, Materials, *Standard Specifications*, Indiana Department of Transportation (INDOT 2020).
15. M. L. Nehdi, J. Sumner, Mater. Struct. **35**, 495-503 (2002)
16. J. M. Shilstone, Concr. Int. **12**, 33-39 (1990)
17. D. N. Richardson, *Report RDT 05-001*, Missouri Department of Transportation (MoDOT 2005)
18. A. Rudy, J. Olek, T. Nantung, R. M. Newell, *Proceedings of the Conf. Dni Betonu* (2008)
19. AASHTO TP-34-99 (2005)